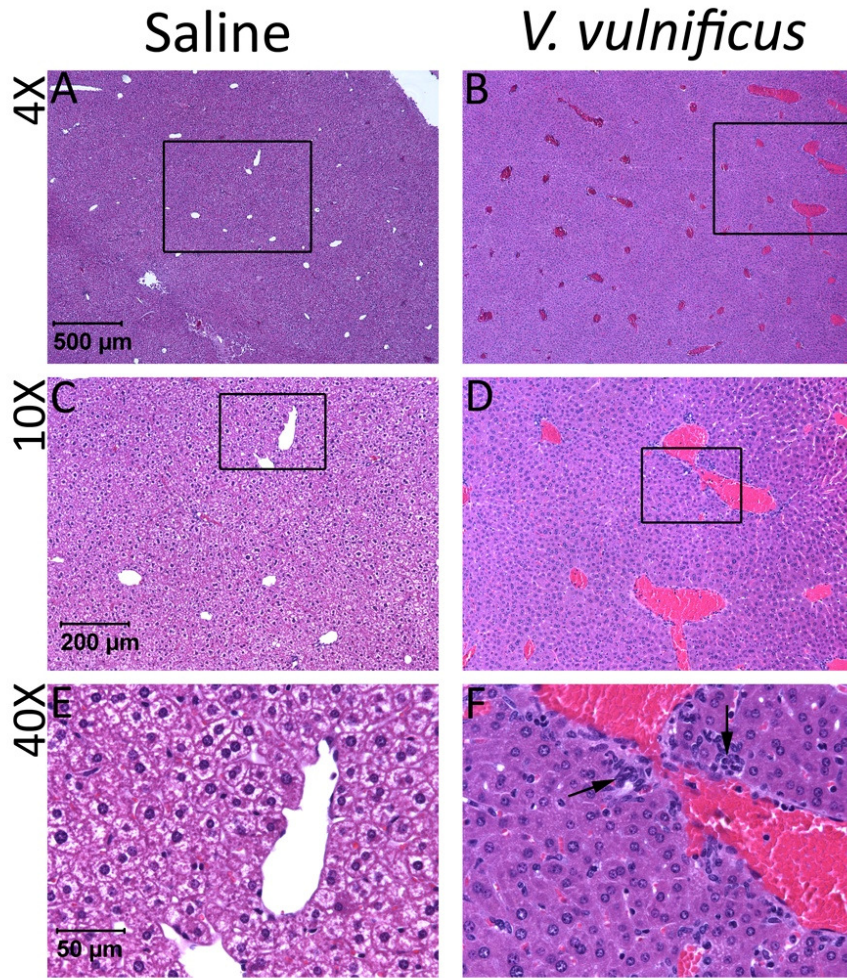
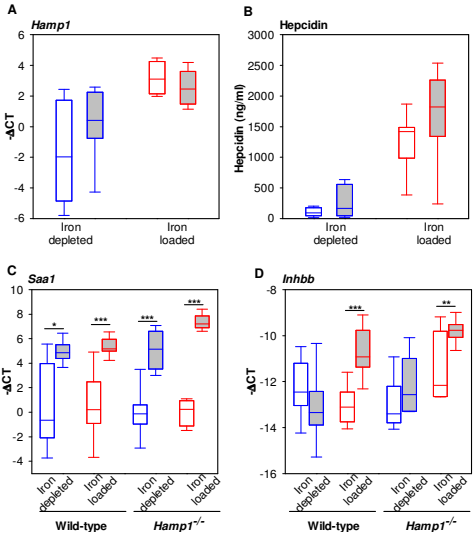


**Figure S1, Related to Figure 1. *V. vulnificus* pathogenicity and growth are greatly enhanced by high iron concentrations. (A)** Kaplan-Meier survival curves for 8-10 week-old WT mice, after s.c. infection with  $1 \times 10^6$  CFU of *V. vulnificus*. Iron-loaded mice (red line) died very rapidly, whereas iron-depleted mice (blue line) survived the infection, with the difference significant at  $p < 0.001$  by log-rank survival analysis. **(B)** Serum was collected from iron-depleted and iron-loaded WT mice. *V. vulnificus* ( $1 \times 10^4$  CFU/ml) was incubated for 3 h at  $37^\circ\text{C}$  with shaking (300 rpm) in LB-N broth (black fill), or in different sera (gray fill) as indicated. Bacterial growth in LB-N broth and low-iron serum ( $26 \mu\text{M Fe}$ ) was similar, but it was greatly increased in high-iron serum ( $60 \mu\text{M Fe}$ ) and in iron-depleted serum supplemented with FAC (added to a final concentration of  $100 \mu\text{M iron}$ ). Bacterial growth was impaired in high iron serum treated with the iron chelator deferiprone ( $150 \mu\text{M}$ ). Protegrin ( $0.4 \text{mg/ml}$ ) addition to high-iron serum killed all the bacteria. Bars represent mean + standard deviation ( $n=7$ ). Statistical significance was assessed using student's *t* test (\*\* $p < 0.01$ ).



**Figure S2, Related to Figure 2. *V. vulnificus* infection causes inflammation and erythrocyte sludging in the liver.** Liver sections (stained with hematoxylin and eosin) of *Hamp1*<sup>-/-</sup> mice injected with saline (A, C, E) or  $1 \times 10^3$  CFU of *V. vulnificus* (B, D, F): rectangular regions are magnified. **(A-D)** Veins and venules in infected mice are dilated and congested with aggregated erythrocytes (B,D), unlike the saline controls (A,C). **(E-F)** Perivascular neutrophil infiltration (arrows) in infected mice (F) but not in saline controls (E).



**E**

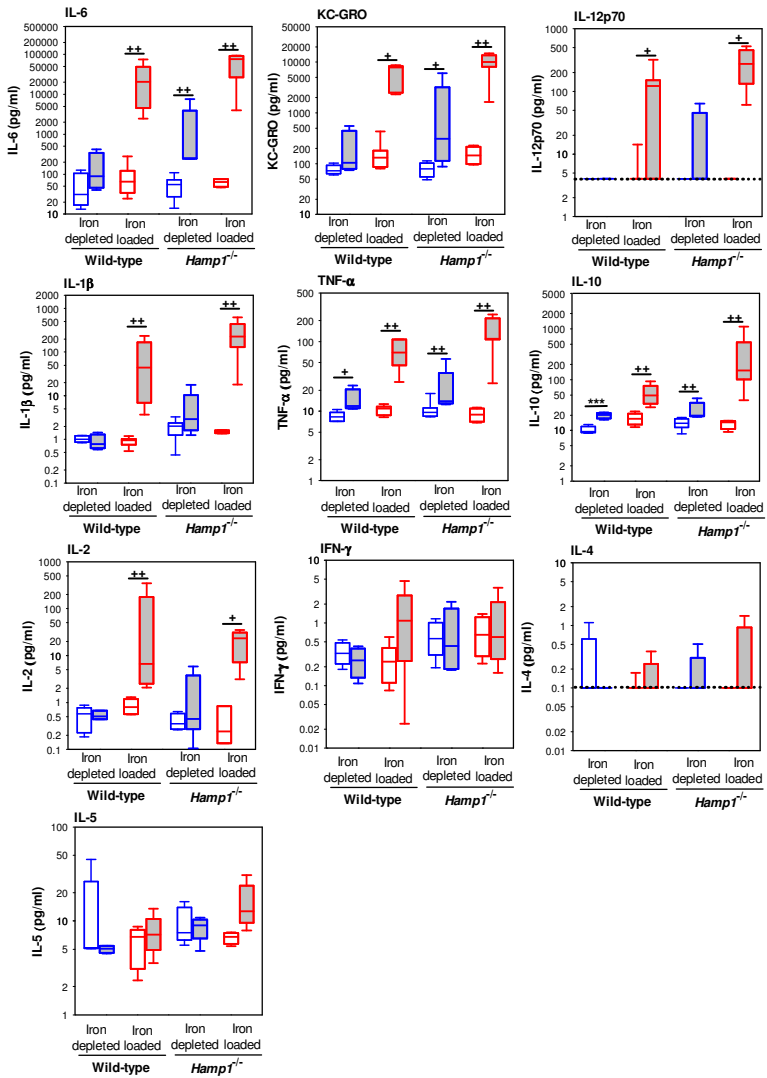


**Figure S3, Related to Figure 3. Liver hepcidin mRNA is no longer significantly increased by 16 h after infection, despite evidence of inflammation.** Iron-depleted (blue) and iron-loaded (red) WT and *Hamp1*<sup>-/-</sup> mice were injected with saline (white fill) or with *V. vulnificus* (grey fill, 10<sup>5</sup> CFU for WT and 300 CFU for *Hamp1*<sup>-/-</sup>), n=6-8 per group. **(A)** Hepatic *Hamp1* mRNA. **(B)** Serum hepcidin. **(C)** Hepatic *Saa1* mRNA. **(D)** Hepatic *Inhbb* mRNA. Measurements of mRNA concentration are shown as -ΔCt relative to actin mRNA. **(E)** A panel of 10 inflammatory cytokines was analyzed in serum from iron-depleted and iron-loaded WT and *Hamp1*<sup>-/-</sup> mice 16 hours after *V. vulnificus* infection (grey bars) or saline injection (white bars). Infected mice presented higher levels of IL-6, KC-GRO, IL-12p70, IL-1β, TNF-α, IL-10 and IL-2. No changes were observed for IFN-γ, IL-4 and IL-5. The black dotted line represents the lower limit of detection of the assay. Statistical significance was assessed using student's *t* test if data were normally distributed (\*p<0.05; \*\*p<0.01; \*\*\*p<0.001) or Mann-Whitney *U* test if they were not (†p<0.05; ††p<0.01), n=6-8 per group.

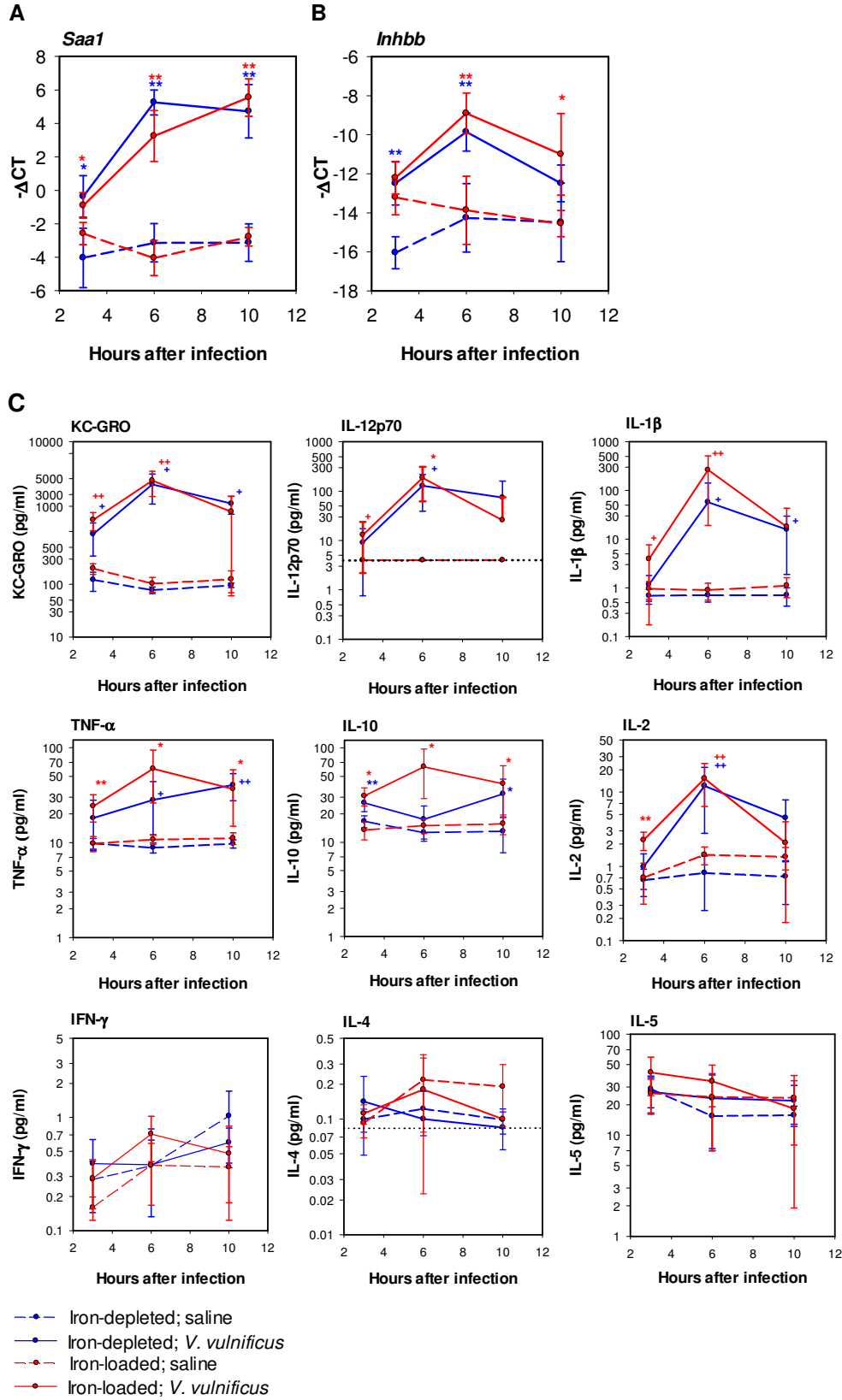


**Figure S4, related to Figure 4. Inflammation is induced early during infection.** qRT-PCR from liver samples was performed to analyze the mRNA expression of *Saa1* (A) and *Inhbb* (B) in iron-depleted (blue) and iron-loaded (red) WT mice, 3, 6 and 10 hours after infection with  $10^5$  CFU *V. vulnificus* (solid lines) or saline injections (dashed lines). All the infected groups increased *Saa1* and *Inhbb* mRNA starting at 3 hours after infection. No differences were observed between iron-loaded and iron-depleted mice. Gene expression results are represented as  $-\Delta\text{Ct}$  relative to actin mRNA. Each dot represents the mean, and error bars represent standard deviation (n=5). (C) A panel of 9 pro-inflammatory cytokines was analyzed in serum from iron-depleted (blue) and iron-loaded (red) WT mice, 3, 6 and 10 hours after *V. vulnificus* infection (solid lines) or saline injection (dashed), n=5 per group. Infected mice presented higher levels of KC-GRO, IL-12p70, IL-1 $\beta$ , TNF- $\alpha$ , IL-10 and IL-2, starting at 3 hours after infection. No changes were observed for IFN- $\gamma$ , IL-4 and IL-5. The black dotted line represents the lower limit of detection of the assay. Statistical significance was assessed using student's *t* test if data were normally distributed (\*p<0.05; \*\*p<0.01 \*\*\*p<0.001) or Mann-Whitney *U* test if they were not (<sup>+</sup>p<0.05; <sup>++</sup>p<0.01).

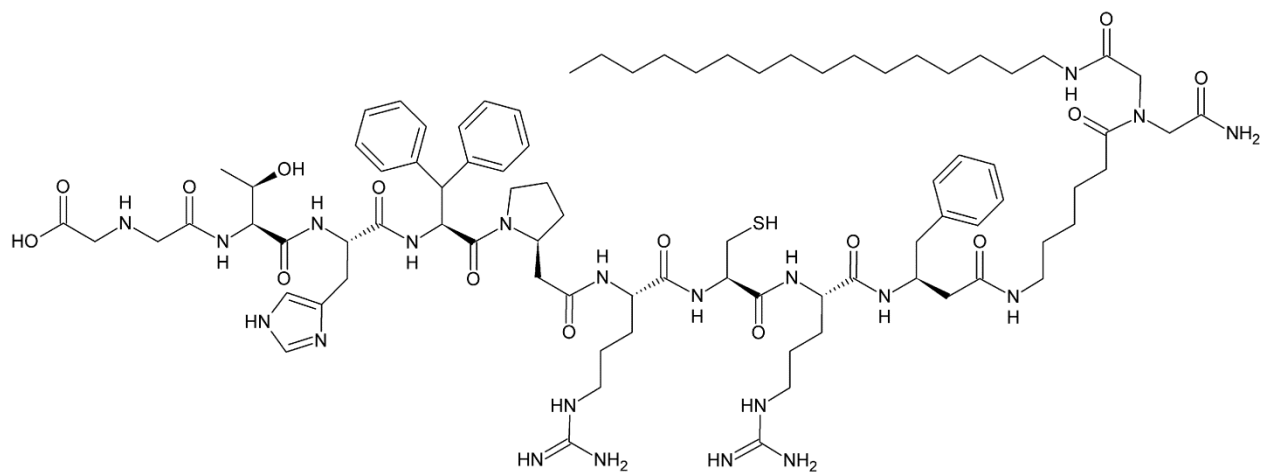


**Figure S5, Related to Figure 5. Molecular structure of minihepcidin PR73.** From N- to C-terminus the primary sequence of PR73 was: iminodiacetic acid, L-threonine, L-histidine, L-3,3-diphenylalanine, L- $\beta$ -homoproline, L-arginine, L-cysteine, L-arginine, L- $\beta$ -homophenylalanine, 6-aminohexanoic acid, iminodiacetic acid palmitylamide (Ida-Thr-His-Dpa-bhPro-Arg-Cys-Arg-bhPhe-Ahx-Ida(NHPal)-CONH<sub>2</sub>).

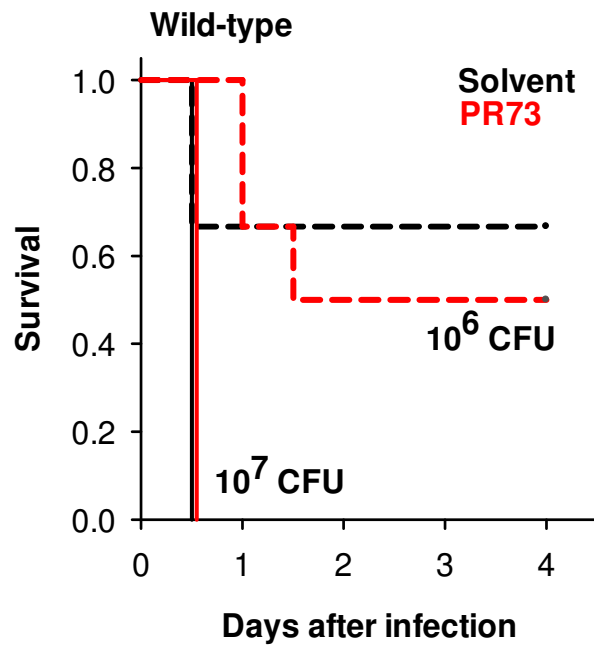


**Figure S6, Related to Figure 6. Minihepcidin does not further protect WT mice from death due to *V. vulnificus* infection.** Kaplan-Meier survival curves for 8-10 week-old WT mice (kept on a standard diet, 270 ppm Fe), treated with minihepcidin PR73 (red lines) or solvent (black lines), 24h and 3h before infection with  $1 \times 10^6$  CFU (dashed lines) or  $1 \times 10^7$  CFU (solid lines) *V. vulnificus*. No statistically significant differences were found between solvent and PR73 treated mice for each bacterial inoculum. N=5-6 per group.



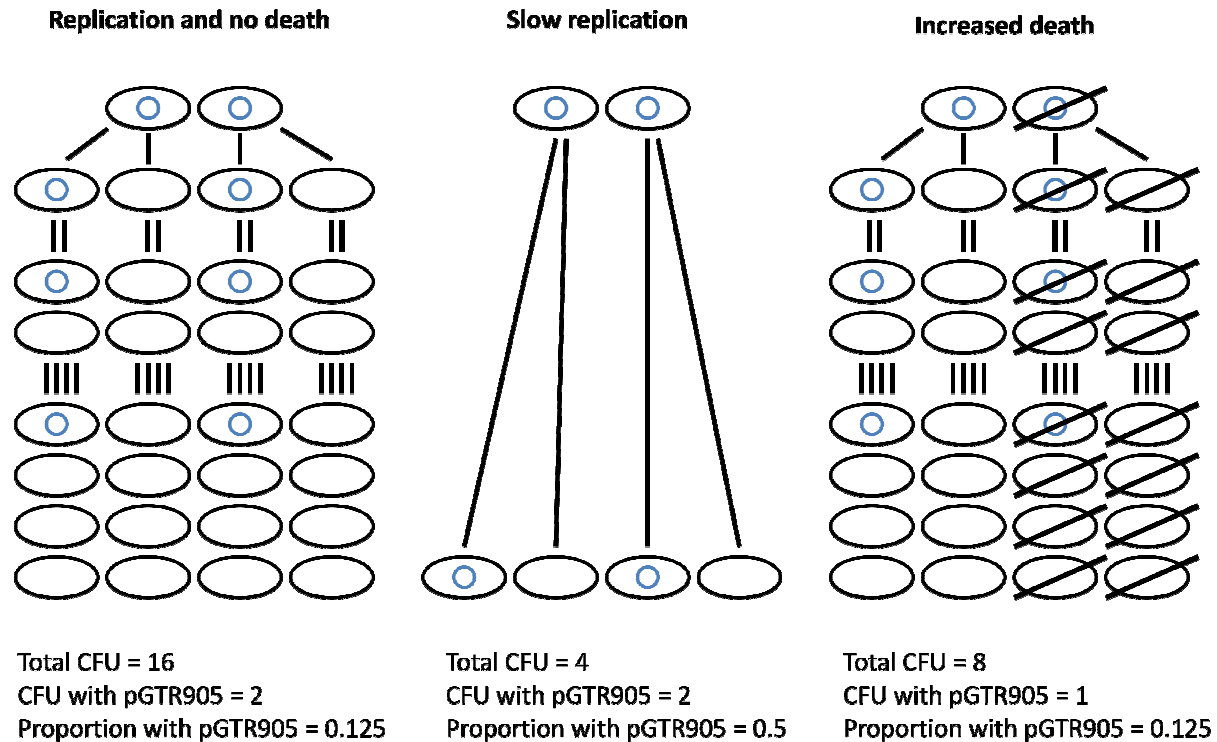


**Figure S7, Related to Figure 7. Use of plasmid pGTR905 to differentiate the replication rate from the death rate of *V. vulnificus* in mouse serum (adapted from Gulig et al, 1997).** The marker plasmid (blue circle) only replicates in the presence of arabinose, which is not present in significant amounts in mouse serum. **Left panel:** under standard conditions (normal replication and no death), a representative population of 2 plasmid-containing bacteria after three divisions yields 16 bacteria, 2 of which contain the plasmid (proportion of plasmid-containing bacteria = 0.125). **Central panel:** if PR73 decreases the replication rate (e.g. only one division occurs within the same time period), the total number of bacteria will be lower (4 CFU) and the proportion of plasmid-containing bacteria will be higher (0.5). **Right panel:** if PR73 increases killing without affecting the replication rate (e.g. half of the bacteria are killed), the total number of bacteria will be lower (8 CFU), but the proportion of plasmid-containing bacteria will be the same as in standard conditions (0.125). Therefore, the total number of bacteria reflects both growth and killing of bacteria whereas the ratio of total to plasmid-containing bacteria reflects growth only.

**Table S1, Related to Figure 1. Serum and liver iron concentrations in WT mice fed an iron-poor (4 ppm Fe) or iron-rich (10000 ppm Fe) diet for 2 weeks (n=8 per group)**

	<b>Serum Fe (<math>\mu\text{M}</math>)</b>	<b>Liver iron (<math>\mu\text{g/g}</math> of wet tissue)</b>
<b>4 ppm diet</b>	38 $\pm$ 9	18 $\pm$ 9
<b>10,000 ppm diet</b>	65 $\pm$ 4	425 $\pm$ 109
<b>p-value</b>	<0.001	<0.001

**Table S2, Related to Figure 7. Serum iron concentrations and bacterial growth in sera *ex vivo***

	Solvent sera		Minihepcidin sera	
	Serum iron	Log <sub>10</sub> (T/P)	Serum iron	Log <sub>10</sub> (T/P)
<b><i>Hamp1</i><sup>-/-</sup> mice, standard diet</b>	66 μM	1.84±0.21	13 μM	0.90±0.02**
<b><i>Hamp1</i><sup>-/-</sup> mice, low-iron diet</b>	64 μM	1.70±0.13	4 μM	0.63±0.53*

Means ± SD are shown. \*p=0.028, \*\*p=0.0017 compared to solvent sera

	High-iron diet		Low-iron diet	
	Serum iron	Log <sub>10</sub> (T/P)	Serum iron	Log <sub>10</sub> (T/P)
<b>WT mice</b>	64 μM	1.75±0.06	37 μM	0.56±0.15*

Means ± SD are shown. \*p=0.0002 compared to high-iron sera